A Stator Turn-Fault Detection Method for Inverter-Fed IPMSM with High-Frequency Current Injection

Myoungho Kim
Power and Control System Division
Samsung Heavy Industries
Hwasung-city, Gyeonggi-do,
South Korea
myungho1.kim@samsung.com

Seung-Ki Sul
Department of Electrical Engineering
& Computer Science
Seoul National University
Seoul, South Korea
sulsk@plaza.snu.ac.kr

Junggi Lee
EV Components Research Group
LG Electronics
Seoul, South Korea
Jungi.lee@lge.com

***Abstract*—This paper presents a turn-fault detection method for inverter-fed Interior Permanent Magnet Synchronous Machines(IPMSMs) using high-frequency current injection when the motor is at standstill. When the motor is stopped, the fault current which flows in the faulty turns and the phase currents can be expressed with the injected phase current and the mutual inductance between each phase winding and the faulty turns. Because of the turn-fault, the injected high frequency currents cause different losses according to the direction of the injection. The proposed detection method exploits the difference of the losses of each case to diagnose the turn-fault. Experimental results are provided to verify the proposed detection method. The resultant loss pattern agrees well with that of the electrical model and shows reasonable sensitivity to the turn-fault. Two-turn fault among 27 turns of a phase winding of the motor under test has been detected easily with existing hardware of the drive system.**

I. INTRODUCTION

The stator winding insulation fault is one of the main sources of the electric machine failure [1]. It has been concerned as an important problem and many studies about the identification of this fault have been conducted to avoid the unexpected breakdown of the machine [1], [2].

The stator winding insulation fault has several forms such as phase-to-phase fault or phase-to-ground fault, however it is generally known that the majority of them results from the turn-fault [3]. Degradation of the insulation system of the winding is caused by combination of many factors like electrical, thermal, mechanical, and environmental stresses. Once insulation between certain turns become broken, the excessive faulty current starts to circulate through the faulty turns and produces excessive heat, which damages further the insulation between windings and causes adverse effects on the turn-fault again. Eventually the damage would propagate and result in phase-to-phase or phase-to-ground fault. Therefore, it is important to detect the turn-fault at its early stage before it develops into a catastrophic failure of the motor.

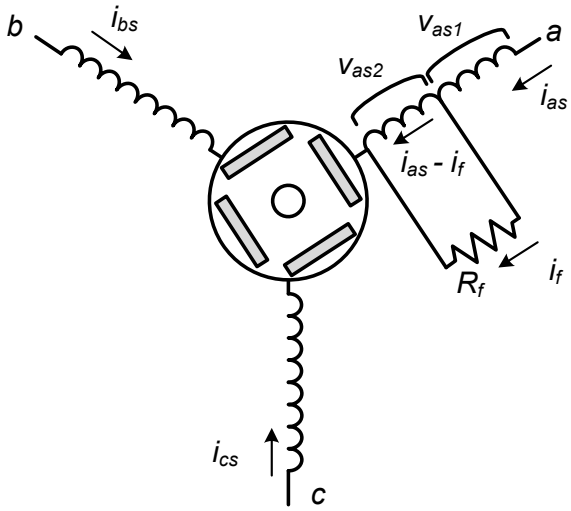

Fig. 1. Schematic circuit of IPMSM with faulted turn in A-phase

Condition monitoring methods to check the insulation status of the motor winding can be categorized into two groups. The first one is the offline test method. The offline tests apply particular ac or dc signal into the motor winding and check the status of the motor winding by observing the responses [1]. These test methods are usually direct and accurate. However, they can be performed only when the motors are disconnected from the service. The second one is online test method, which is able to detect the turn-fault with the motor connected to the system. Most of these methods mainly depend on finding the unbalance of the stator windings. The turn-fault on a specific phase winding makes the impedance of the corresponding phase change, and the impedances of the stator windings become unbalanced. Many online test methods observe certain voltage [4], or current [5], or impedance signature [6], [7] caused by the unbalanced stator winding impedance. However, most of the online test methods focus on utility-fed induction machines and still only a few researched have been conducted for turn-fault detection of inverter-fed

$$\mathbf{v}_s = \mathbf{R}_s\mathbf{i}_s + \frac{d\boldsymbol{\lambda}_s}{dt} = \mathbf{R}_s\mathbf{i}_s + \mathbf{L}_s\frac{d\mathbf{i}_s}{dt} + \omega_r\frac{d\mathbf{L}_s}{d\theta_r}\mathbf{i}_s + \omega_r\frac{d\boldsymbol{\lambda}_r}{d\theta_r}, \tag{1}$$

where $\mathbf{v}_s = \left[v_{as1}\ v_{as2}\ v_{bs}\ v_{cs}\right]^T$, $\boldsymbol{\lambda}_s = \left[(1-\eta)\lambda_{as}\ \eta\lambda_{as}\ \lambda_{bs}\ \lambda_{cs}\right]^T$, $\mathbf{i}_s = \left[i_{as}\ i_{as}-i_f\ i_{bs}\ i_{cs}\right]^T$, $\mathbf{R}_s = diag\left[(1-\eta)R_s\ \eta R_s\ R_s\ R_s\right]$,

$$\mathbf{L}_s = \begin{bmatrix} (1-\eta)L_{ls}+(1-\eta)^2 L_{aa} & \eta(1-\eta)L_{aa} & (1-\eta)M_{ab} & (1-\eta)M_{ac} \\ \eta(1-\eta)L_{aa} & \eta L_{ls}+\eta^2 L_{aa} & \eta M_{ab} & \eta M_{ac} \\ (1-\eta)M_{ab} & \eta M_{ab} & L_{ls}+L_{bb} & M_{bc} \\ (1-\eta)M_{ac} & \eta M_{ac} & M_{bc} & L_{ls}+L_{cc} \end{bmatrix},\quad \boldsymbol{\lambda}_r = \lambda_f\begin{bmatrix} \cos\theta_r \\ \cos\left(\theta_r-\frac{2}{3}\pi\right) \\ \cos\left(\theta_r+\frac{2}{3}\pi\right) \end{bmatrix},$$

where $L_{aa} = L_A - L_B\cos 2\theta_r$, $L_{bb} = L_A - L_B\cos 2\left(\theta_r+\frac{\pi}{3}\right)$, $L_{cc} = L_A - L_B\cos 2\left(\theta_r-\frac{\pi}{3}\right)$,

$M_{ab} = -\frac{1}{2}L_A - L_B\cos 2\left(\theta_r-\frac{\pi}{3}\right)$, $M_{bc} = -\frac{1}{2}L_A - L_B\cos 2\theta_r$, $M_{ac} = -\frac{1}{2}L_A - L_B\cos 2\left(\theta_r+\frac{\pi}{3}\right)$.

machines [4], [7], [8], [9]. Also, most of these methods cannot be used when the motor is at standstill since the fundamental excitation is required to detect the unbalanced characteristic of the stator winding. In addition, inherent asymmetry by imperfect manufacturing is difficult to distinguish from the unbalance by the turn-fault.

Ref. [10] employs high-frequency voltage injection method. It detects the negative sequence component responded by the unbalanced stator winding. This method can be used irrespective of the operating condition, but still suffers from the inherent asymmetry of the machine especially when the motor is at standstill. Especially, in case of IPMSM, it is impossible to distinguish the inherent spatial inductance variation and the unbalance caused by the turn-fault at standstill.

This paper proposes a turn-fault detection method for an inverter-fed IPMSM. The proposed method injects the high-frequency current when the motor is at standstill and diagnoses the turn-fault by the generated loss, which is related to the turn-fault. The proposed method is less sensitive to the inherent asymmetry of the motor and does not require any additional hardware except already existing measuring devices for the motor drive itself. Experiments were conducted to verify the proposed method.

II. Model of IPMSM with Faulty Turns

Fig. 1 presents the schematic of stator windings of turn-faulted IPMSM. The turn-fault is assumed to be occurred in a part of A-phase winding. This assumption is reasonable since practically the turn-fault rarely occur at multiple places concurrently and should be detected before it spreads to other part of the stator winding. In Fig. 1, the A-phase winding can be categorized into two parts: the healthy turns and the faulty turns. The turn-fault is modeled as an additional path across the faulty turns of the winding with fault resistance, R_f. In Fig. 1, v_{as1} and v_{as2} represent the stator voltage of healthy and faulty part of the winding and i_f stands for the fault current, which circulates in the faulty turns. The fraction of the faulty turn in A-phase winding is defined as η.

The schematic in Fig. 1 is interpreted as a four winding motor where the windings are mutually coupled to each other [9]. The electrical model of IPMSM with faulty turns can be derived as (1). In (1), $\boldsymbol{\lambda}_r$, $\mathbf{v}_s$, and $\mathbf{i}_s$ indicate the flux linkage of each winding, the stator voltage, and the current flowing on each winding, respectively. θ_r and ω_r stand for the rotor position and the angular frequency of the rotor. $\mathbf{R}_s$, $\mathbf{L}_s$ represent resistance and inductance matrix and $\boldsymbol{\lambda}_r$ denotes flux linkage originated by the permanent magnet of the rotor. R_s and λ_f are per phase resistance and the magnitude of flux linkage, respectively. Elements of the inductance matrix are composed of self and mutual inductance. L_a indicates the inductance which is independent to the rotor position and L_b indicates the magnitude of the varying inductance according to the rotor position. L_{ls} means the leakage inductance.

III. Proposed Turn-Fault Detection Method

This paper proposes a turn-fault detection method, which injects the high-frequency current into the stator winding and observes the loss generated by it when the motor is at standstill. The loss by the current injection varies according to the condition of the stator winding. Considering only copper loss, the loss in the healthy stator can be expressed as (2). However if there exists a turn-fault in the A phase winding as shown in Fig. 1, the loss equation varies as (3).

$$P_{e\_healthy} = \frac{1}{2}R_s\left(I_{as}^2 + I_{bs}^2 + I_{cs}^2\right), \tag{2}$$

$$P_{e\_faulty} = \frac{1}{2}R_s\left\{(1-\eta)I_{as}^2 + I_{bs}^2 + I_{cs}^2\right\} + \frac{1}{2}\left\{\eta R_s\left(I_f - I_{as}\right)^2 + R_f I_f^2\right\}, \tag{3}$$

where I_{as}, I_{bs}, I_{cs} and I_f denote magnitudes of each phase current and the fault current. If turn-fault occurs, the fault current is induced by the injected phase current and it

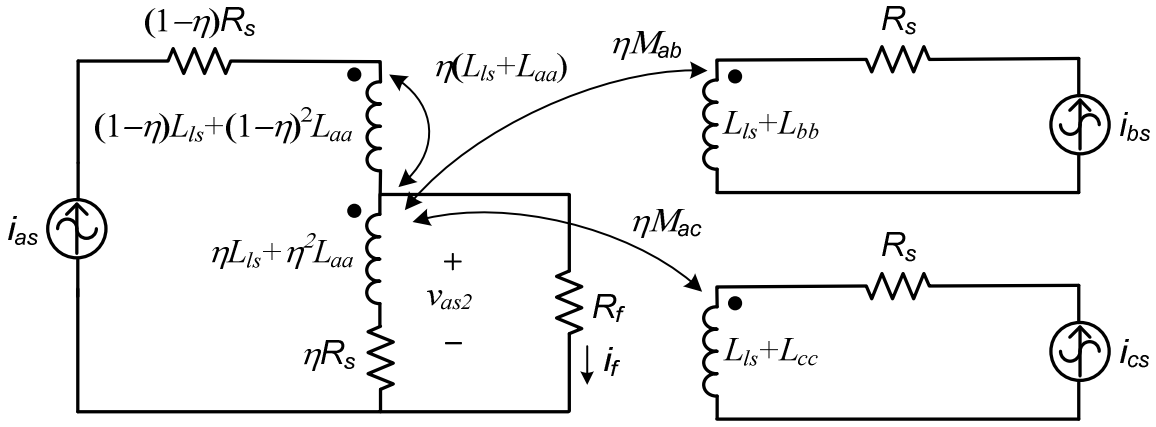

Fig. 2. Equivalent circuit of stator windings with faulted turn in a phase

increases the loss. Using this characteristic, the level of the loss can be employed as an indicator of turn-fault. It is possible to compare the loss at each diagnosis process with the pre-measured loss data to detect the turn-fault. However, that method might be sensitive to the operating condition since the resistance of the stator winding and the loss of semiconductors vary according to the temperature.

In order to avoid this problem, this paper exploits the power loss variation according to the phase of the injected current vector. The injected current reference in the d-q stationary reference frame is shown in (6).

$$\mathbf{i}_{dqs}^{s*} = \left(I_{inj}\cos\omega_{inj}t\right)e^{j\theta_{inj}},\ \theta_{inj} = 0,\ \frac{2}{3}\pi,\ \frac{4}{3}\pi, \tag{4}$$

where I_{inj} and ω_{inj} is the magnitude and the frequency of the injected current. The phase of the injected current vector, θ_{inj}, is 0, 2/3π, 4/3π which means the current is injected into the direction of the A, B and C-phase successively.

Theoretically, the loss should be identical and independent to θ_{inj} if there is no turn-fault. However, if the turn-fault exists in a particular phase winding, the loss becomes different according to the injecting direction, θ_{inj}. Therefore the turn-fault can be diagnosed by this loss difference. The loss difference by the turn-fault can be explained with the electrical model of the turn-faulted PMSM model. When the rotor is not rotating, the voltage model shown in (1) can be simplified as (5) and the voltage across the faulty turns is derived as (6).

$$\mathbf{v}_s = \mathbf{R}_s\mathbf{i}_s + \frac{d\boldsymbol{\lambda}_s}{dt} = \mathbf{R}_s\mathbf{i}_s + \mathbf{L}_s\frac{d\mathbf{i}_s}{dt}, \tag{5}$$

$$\begin{aligned} v_{as2} &= R_f i_f \\ &= \eta R_s\left(i_a - i_f\right) - \left(\eta L_{ls} + \eta^2 L_{aa}\right)\frac{di_f}{dt} + \eta\left(L_{ls}+L_{aa}\right)\frac{di_{as}}{dt} \\ &\quad + \eta M_{ab}\frac{di_{bs}}{dt} + \eta M_{ac}\frac{di_{cs}}{dt}. \end{aligned} \tag{6}$$

Eq. (6) shows the relationship between the three phase currents and the fault current. Assuming three phase currents are controlled, the voltage model (6) can be modeled as a current model as shown in Fig. 2. In Fig. 2, the phase currents are modeled as variable ac current sources and the fault current is induced by the phase currents and the mutual inductance between each phase winding and the faulty turns. The fault current can be represented by the phase currents and the circuit parameters by applying the Laplace transform to both sides of (6) and it can be rearranged as (7).

$$\begin{aligned} I_f(s) = &\frac{\eta}{s\left(\eta L_{ls} + \eta^2 L_{aa}\right) + \eta R_s + R_f} \\ &\times\left[\left\{s\left(L_{ls}+L_{aa}\right) + R_s\right\}I_{as}(s) + sM_{ab}I_{bs}(s) + sM_{ac}I_{cs}(s)\right]. \end{aligned} \tag{7}$$

Eq. (7) shows that the induced fault current would be different according to the phase currents and the mutual inductance between each phase winding and the faulty turns. The proposed detection method exploits this feature. The high-frequency current is injected into different phases, which results in different fault currents and different power losses.

The induced fault currents and power losses are calculated using (7) and (3) and presented in Fig. 3 and Fig. 4 when I_{inj} and ω_{inj} set to 3.5 A and 2513 rad/s. An IPMSM is used for the calculation and its parameters are listed in Table I. R_f and η is set to 20 mΩ and 1/27 (one turn-fault).

Fig. 3 shows that the magnitude of the fault current is the largest when θ_{inj} is 0 rad. This is because the mutual inductance between the A-phase winding and the faulty turns is largest among those between one phase winding and the faulty turns ($L_{ls} + L_{aa} > M_{ab}, M_{ac}$) since the faulty turn is located in the A-phase. It means that the fault current is maximized when the current is injected into the phase where the turn-fault occurs.

The magnitude of the fault current is also different according to the rotor position since the mutual inductance

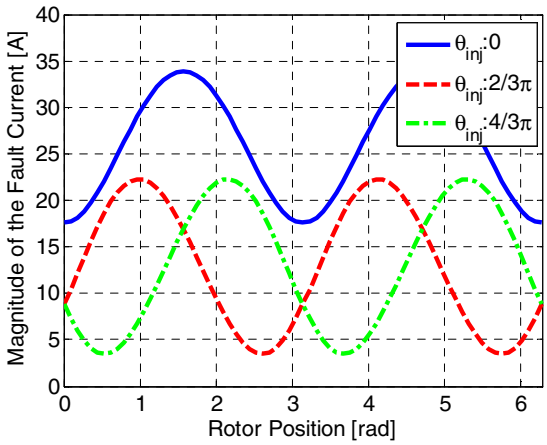

Fig. 3. Calculated fault current by the current injection

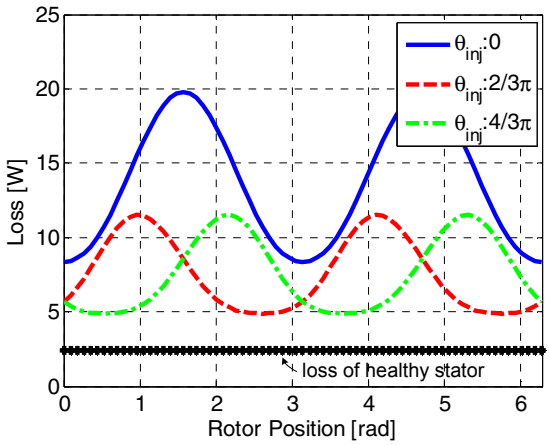

Fig. 4. Calculated loss by the current injection

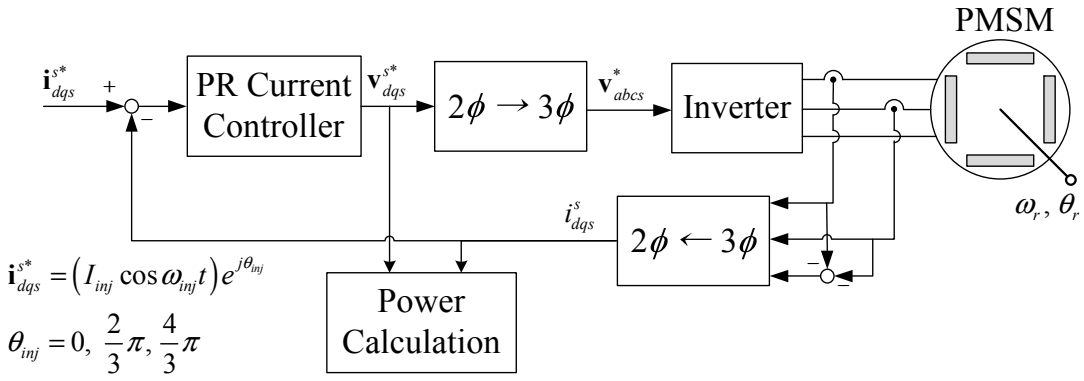

Fig. 5. The proposed turn-fault detection scheme

between each phase windings and the faulty turns varies with the rotor position. However, still the magnitude of the fault current is maximized when θ_{inj} is 0 rad.

Fig. 4 shows the calculated loss according to the position of the rotor and the angle of the injected current, θ_{inj}. The loss of the healthy stator without turn-fault is the lowest since no fault current is induced. Also, the loss of this case is constant irrespective of θ_{inj} and the rotor position as the mutual inductance does not affect the copper loss of the healthy stator winding. Whereas, the loss is directly related to the fault current when the turn-fault exists. The loss become higher as the magnitude of the fault current gets larger, thus the loss is maximized when θ_{inj} is 0 rad.

The turn-fault detection is achieved by comparing the loss caused by the current injection into three different θ_{inj}. If turn-fault exists in a specific phase winding, the loss would be different according to θ_{inj}. The difference between the minimum loss and the maximum loss is used as an indicator of the turn-fault. The location of the turn-fault also can be known since the loss is maximized when the current is injected to the phase where the turn-fault occurs.

Fig. 5 shows the proposed turn-fault detection scheme. When a motor is at standstill, the high-frequency current is injected into three phase windings by a PR (Proportional and Resonant) controller. The loss of each case is calculated with the measured current and the voltage reference of the PR controller. If the difference between the maximum loss and the minimum loss exceeds certain threshold, the motor is considered to have faulty turns.

IV. Experimental Results

The proposed method was verified by experiments. An IPMSM was employed as a test motor whose parameters are the same as the values used for the calculation, as shown in Table I. The test motor was modified to emulate the turn-fault condition. Additional taps were built on the stator windings so that some internal turns of the stator windings could be accessible externally. By connecting them, turn-fault could be emulated. The winding configuration of the test motor is shown in Fig. 6. The proposed detection method was implemented using a commercial DSP and an IGBT inverter, which is already used for the motor drive.

Fig. 7 shows the current waveforms while the rotor was stopped at -0.09 rad. Three turns of the A-phase winding is shorted externally and the high-frequency current was injected into three phases successively as shown in Fig. 5. I_{inj} and ω_{inj} set to 3.5 A and 2513 rad/s. Fig. 7 (a) shows the variation of three phase currents and fault current according to θ_{inj}. The A, B, and C-phase current were largest when the

TABLE I. IPMSM PARAMETERS

Quantity	Value [Unit]
Rated Power	7 [kW]
Phase resistance	R_s ; 0.265 [Ω]
Inductance	L_d ; 4.00 [mH] L_q ; 7.22 [mH]
# of turns per phase	27
Rated current	23.8 [A_{peak}]

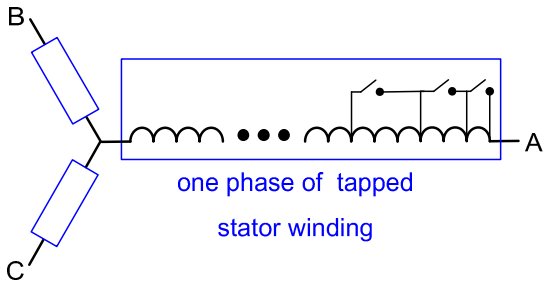

Fig. 6. The winding configuration of the test motor

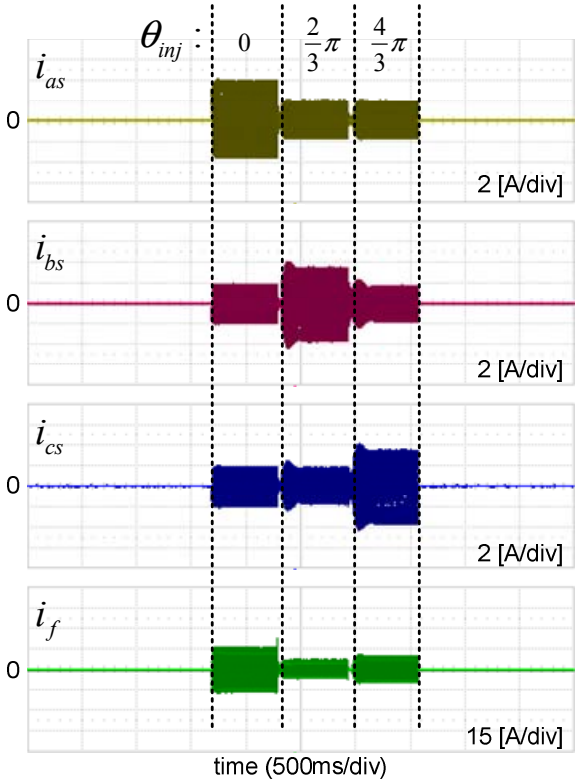

(a) phase current and fault current according to θ_{inj}

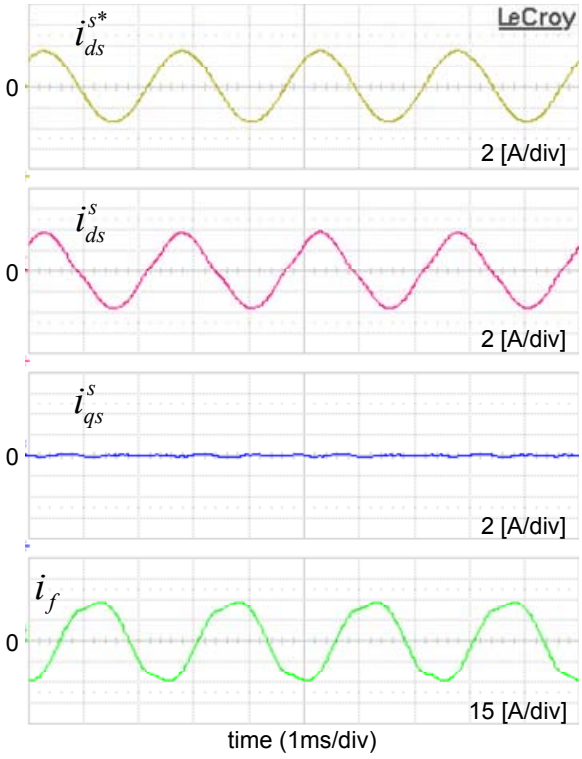

(b) d and q-axis current and fault current when θ_{inj} = 0 rad

Fig. 7. Current waveforms with faulty turns

θ_{inj} is 0, 2/3π, 4/3π each. Since the faulty turns were located at the A-phase, the magnitude of the fault current was largest when θ_{inj} is 0 rad. In the experiments, the fault current was measured for only monitoring purpose and was not used for the turn-fault detection algorithm. Fig. 7 (b) shows the d and q-axis current in the stationary reference frame and the fault current when θ_{inj} was 0 rad. Since θ_{inj} was 0 rad, the q-axis current reference was zero and only sinusoidal d-axis current is injected. Little amount of harmonics on the currents seemed to be caused by model discrepancy by faulty turns. The shape of fault current was not sinusoidal because it was not controlled but induced by the injected current.

Fig. 8 shows the resultant loss with three turns of the A phase winding shorted. It shows an analogous tendency to the calculate d loss shown in Fig. 4. The loss when θ_{inj} is 0 rad is larger than that of other cases, and the test motor can be diagnosed as turn-faulted with this fact. However, the loss difference varies according to the rotor position. For the case that the diagnosis ought to be performed without rotating the rotor, the worst condition was checked. Fig. 9 shows the least loss differences for different faulty turns (The rotor position is around 0 or π rad where the loss difference according to the turn-fault is minimized). The extent of the least loss difference gets larger enough as the fault level intensifies. Accordingly, the proposed method can be used for the turn-fault detection. In the case of 1 turn fault among 27 turns, the loss difference at th e worst condition is 1.3 W and it reveals almost 1 W difference with healthy motor. The rated power of the motor under test is 7 kW, and with the resolution of current sensors and DC link voltage sensor 1 W is the border line of the detection. While, in the case of 2 turn faults, the difference is more than 2 W and it can be easily detected.

Fig. 8. Loss caused by current injection according to the rotor position

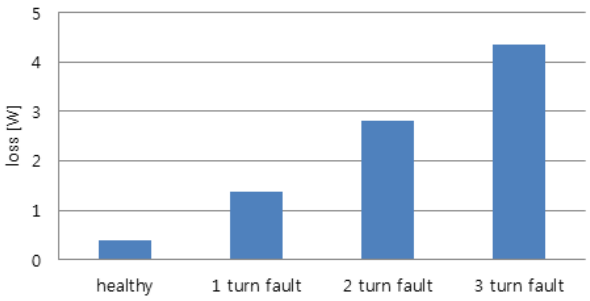

Fig. 9. Least loss difference versus the number of faulty turns

V. CONCLUSION

A turn-fault detection method has been proposed in this paper. The proposed method is used for inverter-fed IPMSM drive system when the motor is at standstill. The turn-fault in a specific phase winding causes additional current path in the winding. When the motor is at standstill, the fault current circulating in this path is determined by the phase currents and the mutual inductance between each phase winding and the faulty turns. The proposed detection method injects the high-frequency current into the stator windings with three directions successively and examines the generated loss of each case. If the turn-fault exists, the magnitudes of the fault currents would be different according to the injected directions, which results in the different losses. This loss difference is used as a turn-fault indicator. The injected current is controlled by a PR controller and the loss is calculated with the measured current and the voltage reference of the controller. The proposed detection method was verified with experiments. An IPMSM was used with the stator winding modified to emulate the turn-fault condition. The loss pattern caused by the high-frequency current injection shows the similar tendency to the calculated one and the loss difference according to the injected directions was enough to diagnose the turn-fault. In the case of the tested motor, two turn fault among 27 turns of the motor under test has been detected easily with existing hardware of the drive system.

REFERENCES

[1] Grubic, S.; Aller, J.M.; Bin Lu; Habetler, T.G., "A Survey on Testing and Monitoring Methods for Stator Insulation Systems of Low-Voltage Induction Machines Focusing on Turn Insulation Problems," *Industrial Electronics, IEEE Transactions on* , vol.55, no.12, pp.4127,4136, Dec. 2008

[2] Nandi, S.; Toliyat, H.A.; Xiaodong Li, "Condition monitoring and fault diagnosis of electrical motors-a review," *Energy Conversion, IEEE Transactions on* , vol.20, no.4, pp.719,729, Dec. 2005

[3] Bellini, A.; Filippetti, F.; Tassoni, C.; Capolino, G.-A., "Advances in Diagnostic Techniques for Induction Machines," *Industrial Electronics, IEEE Transactions on* , vol.55, no.12, pp.4109,4126, Dec. 2008

[4] Tallam, R.M.; Habetler, T.G.; Harley, R.G., "Stator winding turn-fault detection for closed-loop induction motor drives," *Industry Applications, IEEE Transactions on* , vol.39, no.3, pp.720,724, May-June 2003

[5] Kliman, G.B.; Premerlani, W.J.; Koegl, R.A.; Hoeweler, D., "A new approach to on-line turn fault detection in AC motors," *Industry Applications Conference, 1996. Thirty-First IAS Annual Meeting, IAS '96., Conference Record of the 1996 IEEE* , vol.1, no., pp.687,693 vol.1, 6-10 Oct 1996

[6] Trutt, F.C.; Sottile, J.; Kohler, J.L., "Online condition monitoring of induction motors," *Industry Applications, IEEE Transactions on* , vol.38, no.6, pp.1627,1632, Nov/Dec 2002

[7] Siwei Cheng; Pinjia Zhang; Habetler, T.G., "An Impedance Identification Approach to Sensitive Detection and Location of Stator Turn-to-Turn Faults in a Closed-Loop Multiple-Motor Drive," *Industrial Electronics, IEEE Transactions on* , vol.58, no.5, pp.1545,1554, May 2011

[8] P. Garcia, F. Briz, M. W. Degner, and A. B. Diez, "Diagnosis of induction machines using the Zero sequence voltage," *in Rec. of Conf. IEEE IAS*'04, pp 735-742, Seattle, Washington, USA, October, 2004

[9] Youngkook Lee, "A stator turn fault detection method and a fault tolerant operating strategy for interior PM synchronous motor drives in safety-critical applications," Ph. D dissertation, Georsia Institue of Technology, 2007.

[10] Briz, F., Degner, M.W., Zamarron, A. and Guerrero, J.M., "On-line stator winding fault diagnosis in inverter-fed AC machines using high frequency signal injection," *IEEE Trans. Ind. Appl.*, vol. 39, no. 4, pp. 1109-1117, Jul./Aug. 2003.